Int. J. Environ. Sci. Technol. (2015) 12:571–580
DOI 10.1007/s13762-013-0462-2

ORIGINAL PAPER

Characteristics, kinetics and thermodynamics of Congo Red biosorption by activated sulfidogenic sludge from an aqueous solution

K. Rasool · D. S. Lee

Received: 15 February 2013 / Revised: 22 November 2013 / Accepted: 26 November 2013 / Published online: 14 December 2013

Abstract The kinetics and thermodynamics of the biosorption of textile dye Congo Red on anaerobic activated sulfidogenic sludge were examined. The influence of different adsorption parameters such as pH, temperature, contact time and initial dye concentrations on the biosorption capacity was also investigated. The sulfidogenic sludge showed a maximum biosorption density of 238.90 mg dye/g cell for Congo Red at an initial dye concentration of 1,000 mg/L, pH 3.5 and 22 °C, which is higher than that of many other adsorbents reported in the literature. The biosorption processes obeyed the Langmuir isotherm and exhibited pseudo-second-order rate kinetics. The thermodynamic parameters indicated the spontaneous and exothermic nature of Congo Red biosorption. The Fourier transform infrared spectra revealed the dye interaction with the biomass. Scanning electron microscopy showed significant changes in the surface morphology of the sludge after dye biosorption. These results showed that sulfidogenic sludge biomass is an attractive alternative low-cost biosorbent for the removal of the dye from aqueous media.

Keywords Biosorption · Congo Red · Isotherms · Thermodynamics · Sulfidogenic sludge

K. Rasool · D. S. Lee (✉)
Department of Environmental Engineering, Kyungpook National University, 80 Daehak-ro, Buk-gu, Daegu 702-701, Republic of Korea
e-mail: daesung@knu.ac.kr

Introduction

The effluent from many industries such as textiles, paper, printing, cosmetics contains a considerable amount of hazardous dyes. A small amount of dye in water is visible. The discharge of dye-containing wastewater into water bodies not only has esthetic impacts but can also affect aquatic life because several dyes are toxic, mutagenic or carcinogenic (Weisburger 2002). Therefore, the removal of dyes is one of the most difficult requirements faced by these industries. Azo dyes comprise more than 60 % of dyes applied globally in the textile industry (Isik and Sponza 2005). Anionic reactive and acid dyes are water soluble and are the most problematic. Hence, it is difficult to remove them via conventional wastewater treatment systems.

The biosorption of hazardous contaminants is an attractive technology for the treatment of municipal and industrial wastewater for the removal of dyes. A large number of low-cost biosorbents, including fungal biomass, yeast, algal biomass, plant waste, fiber, fruit waste, chitosan and agricultural wastes, have been evaluated for the removal of dyes from wastewater (Chatterjee et al. 2007; Han et al. 2008). On the other hand, there has been continuous investigation aimed at developing better and more easily available biological materials.

Among the many low-cost biosorbents available, aerobic and anaerobic activated sludge used for the domestic and industrial wastewater treatment is one of the most economical and abundantly available materials with millions of tons produced annually worldwide. Activated sludge is an attractive novel biosorption material. The free availability and high biosorption capacity of activated sludge have been attributed to the presence of a large number of binding sites on the cell walls of microbes

because they are composed mainly of polysaccharides, proteins and lipids. Over the past few years, several studies have reported the potential for applying dried aerobic and anaerobic sludge for the biosorption of dyes and other hazardous materials from different effluents (Caner et al. 2009; Ju et al. 2008; Otero et al. 2003). In recent years, a few researchers have examined the potential of living anaerobic activated sludge biosorption for the treatment of effluent (Qiu et al. 2012; Wang et al. 2006).

In wastewater treatment plants, anaerobic sludge combines the advantages of biosorption and biodegradation, which increase the removal efficiency. Although there has been increasing research on anaerobic dye degradation, little is known about the biosorption capability and mechanism of biosorption. Information on the biosorption of pollutants to anaerobic sludge is important not only for the removal of pollutants themselves, but also for modeling biological treatment systems (Qiu et al. 2012). Accordingly, there is a need for further study to evaluate the potential of the most easily available and commonly used activated anaerobic biomass to remove dye stuffs and determine the mechanism for the biosorption process. Anaerobic sulfate-reducing bacterial (SRB) communities are commonly observed in activated sludge used to treat sulfate-rich textile wastewater (Rasool et al. 2013). To the best of the authors' knowledge, there are no reports on the biosorption of dyes onto SRB sludge.

This study examined the biosorption potential of SRB sludge for the removal of benzidine-based anionic diazo textile dye Congo Red (CR) from an aqueous solution. The performance of SRB sludge as a new absorbent for CR removal under different operating conditions was investigated, and the experimental results were analyzed using kinetic, equilibrium and thermodynamic models. The present work was carried out at Kyungpook National University in Republic of Korea from March 2012 to January 2013.

Materials and methods

Preparation of biosorbent and dye solution

The mixed culture of SRB used in this study was enriched from the anaerobic digester sludge at a municipal wastewater treatment plant in South Korea. Postage's B medium was used to prepare the active SRB cultures (Postgate 1984). This medium contained (in g/L) K_2HPO_4 0.5, NH_4Cl 1.0, $CaSO_4$ 1.0, $FeSO_4{\cdot}7H_2O$ 0.5, sodium lactate 3.5, $MgSO_4{\cdot}7H_2O$ 2.0, yeast extract 1.0, ascorbic acid 0.1 and thioglycollic acid 0.1. Sodium sulfate and sodium lactate were used as the sulfate and carbon sources, respectively. The pH of the medium was initially adjusted to approximately 7.5 with a 1-N NaOH solution and heat-sterilized at 15 psi and 120 °C for 20 min. The medium was purged with high-purity nitrogen gas to maintain the anaerobic conditions before inoculating. The culture was maintained in 1-L bottles at 35 °C on a rotary shaker at 110 rpm. The developed culture was subcultured further each week. Blackening of the media indicated sulfate reduction and sulfide production. The biomass was harvested in the growing stage and washed thoroughly with distilled water to remove the surface soluble ions. This process was repeated three times to confirm the effective washing of the biomass and was finally used for biosorption studies, giving volatile suspended solids (VSS) concentration of 9.0 g/L. The sulfidogenic biomass was stored in refrigerator at 4 °C until needed.

CR dye was purchased from Sigma-Aldrich (South Korea) and used as received. The stock solution (1,000 mg/L) was prepared by dissolving the required amount of dye in distilled water and stored in a refrigerator at 4 °C until needed. The test solutions of the desired concentrations were prepared by diluting the stock solution with distilled water.

Batch experiments

The batch biosorption experiments were carried out in 250-mL glass Erlenmeyer flasks. All the batch experiments were performed by adding 5 mL of anaerobic SRB sludge to 100 mL of the dye solution containing 100 mg/L CR. Batch studies were performed at a constant initial pH of 3.5 and 110 rpm under a controlled temperature of 22 °C in a shaking incubator. The pH was adjusted using 0.1 M NaOH and 0.1 M HCl solutions. The effect of temperature on the biosorption capacity was examined over the temperature range 22–50 °C. The effect of the dye concentrations on the biosorption capacity was examined by varying the initial dye concentrations (100, 200, 300, 500, 700 and 1,000 mg/L). Equilibrium studies were carried out for 150 min to determine the equilibrium time. The samples were taken at pre-determined time intervals and centrifuged at 5,000 rpm for 10 min. The supernatant was used to analyze the residual dye in solution. All the studies were performed in triplicate, and the mean values are reported.

Analytical methods

The concentration of dye before and after biosorption was determined by UV–vis spectroscopy (Hitachi U-2800) at the maximum visible absorbance wavelength of the dye

(498 nm). Decolorization was quantified by correlating the absorbance at this wavelength. The dye adsorbed by the sludge biomass was calculated from the difference between initial concentration and the final concentration in the supernatant and was calculated using the following equation:

$$q_e = \frac{C_i - C_f}{m} V \quad (1)$$

where C_i and C_f are the initial and final dye concentrations, respectively. V is the volume of the dye solution (L) and m is the mass of the sludge biomass used as VSS (g), which were determined according to the Standard Methods (APHA 1998). Point of zero charge (PZC) of anaerobic SRB sludge was determined by solid addition method as described earlier (Ofomaja et al. 2009).

Surface morphology characterization and FTIR analysis

Scanning electron microscopy (SEM, Hitachi S-4300 (Japan)) was performed to observe the morphology and surface structure of the sludge biomass before and after dye biosorption. SEM imaging of the samples was accomplished using the following procedure. The cells were fixed with 2 % glutaraldehyde for 24 h at room temperature followed by washing with 0.1 M phosphate buffer (pH 7.4). The samples were then allowed to dry completely for 2 days at room temperature and were then coated with platinum by sputtering.

Sulfidogenic biomass functional groups, the presence of binding sites and their involvement in biosorption were investigated by Fourier transform infrared (FTIR, Spectrum 100, Perkin Elmer, USA) spectroscopy. For the sludge sample, 10 mL of the sample at equilibrium after biosorption was taken and centrifuged at 5,000 rpm for 10 min. The clear supernatant was wasted, and the sludge biomass was used for FTIR analysis. The FTIR spectra of the SBR sludge before and after biosorption were recorded over the region 400–4,000 cm^{-1}, with the samples prepared as KBr pellets at high pressure.

Results and discussion

Effect of pH

CR changes its color from red to dark blue at pH $\leq$ 2, and the original red color is different at pH $>$ 10 (Somasekhara et al. 2012). CR undergoes a protonation process in acidic solutions due to binding of cations to the unshared electron pairs of nitrogen atoms of the naphthyl and azo groups of the dye. The protonation process results in two different resonance structures of ammonium and azonium ions (Bonancêa et al. 2006). The initial pH of the dye solution has a significant effect on the maximum visible absorbance wavelength below pH 3.5, but no chemical structural change in dye molecules occurs over the pH range 3.55–10.95 (Sara and Tushar 2012). In this study, the effect of the initial solution pH on adsorption was examined in the range 3.5–10. Adsorption of the dye decreased from 82.64 to 35.63 mg dye/g cell with increasing initial pH from 3.5 to 10. The effective pH was found to be 3.5 and was used in further studies. PZC of SRB sludge was found to be at pH 2.8. The overall surface charge on the sludge biomass became positive when pH was lower than PZC of the biomass. At low pH, the surface of the anaerobic SRB sludge acquired a positive charge by adsorbing abundant H^+ ions from the acidic solution. As CR is an acidic dye and contains a negatively charged sulfonated group ($–SO_3–Na^+$), a significantly strong electrostatic attraction appears between the negatively charged dye molecules and positively charged surface sites. At higher pH, excessive hydroxyl ions may compete with the dye anions for the positively adsorption sites, which causes a decrease in biosorption capacity. This phenomenon was also observed for the biosorption of CR on the coir pith, waste orange peel and the pine cone powder (Namasivayam et al. 1996; Sara and Tushar 2012). On the other hand, significant adsorption of the anionic dye on the anaerobic SBR sludge still occurred at alkaline pH. This suggests that the chemisorption mechanism might be operative (Namasivayam et al. 1996).

Effect of the contact time and initial dye concentration

The effect of the contact time on the adsorption of CR dye was examined at different initial dye concentrations (Fig. 1). The adsorption of CR on the SRB increased with increasing contact time, and equilibrium was reached within 70 min. The high removal rate at the start of the contact time was attributed to the large number of vacant binding sites available for the adsorption of CR. As the exterior surface became exhausted, the dye uptake rate began to decrease, and finally an apparent equilibrium was reached within 70 min depending on the initial dye concentrations. This relatively short contact time might also provide an advantage for the large-scale application of the adsorption method to real wastewater treatment plants. The dye adsorption density increased from 82.64 to 238.90 mg dye/g cell, with increase in the initial CR concentration was increased from 100 to 1,000 mg/L. Thus, the equilibrium removal of CR decreased from 79.80 to 23.08 %. There-

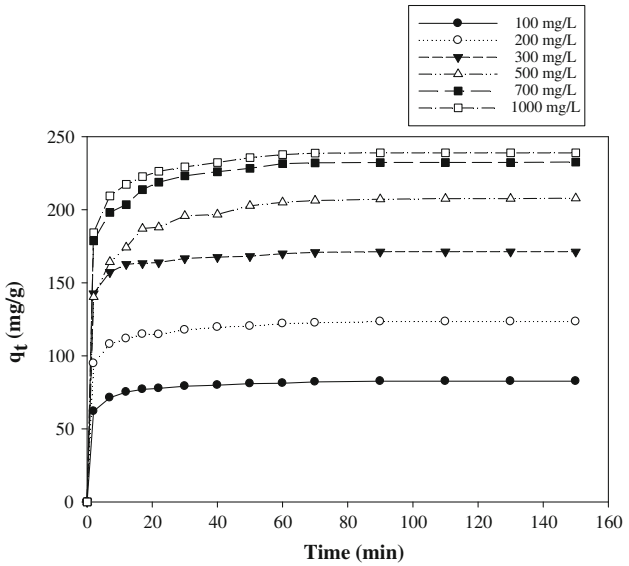

Fig. 1 Equilibrium time profile for the biosorption of CR on SRB sludge at different initial dye concentrations (initial pH = 3.5, 22 °C, 110 rpm)

Table 1 Comparative study of CR biosorption (C_i = 100 mg/L) on SRB sludge with other low-cost adsorbents

Adsorbents	pH	Adsorption capacity (mg/g)	References
Eggshells	6.0	69.45	Saha et al. (2011)
Fly ash	5.0	9.61	Acemioğlu (2004)
Ca-bentonite	6.92	45.0	Lian et al. (2009)
Cashew nut shell	3.0	5.184	Senthil et al. (2010)
Jujuba seeds	2.0	34.64	Somasekhara et al. (2012)
Sugarcane bagasse	5.0	10.0	Zhang et al. (2011)
Anaerobic SRB sludge	3.5	82.64	This study

fore, the initial dye concentration has a significant effect on its removal from aqueous solution. A high initial dye concentration could result in a high mass gradient pressure between the solution and adsorbent, which provides a driving force to overcome the resistance to mass transfer between the aqueous and solid phase (Toor and Jin 2012; Vimonses et al. 2009). The biosorption density of CR by the SRB sludge in this study was compared with those obtained in previous studies of CR biosorption at the initial dye concentration of 100 mg/L using different low-cost biosorbents (Table 1). The adsorption capacity of the anaerobic SRB sludge was higher than that of most adsorbents reported previously. Therefore, SRB sludge is considered to be an excellent adsorbent for the removal of CR.

Effect of temperature and thermodynamic analyses

To examine the effect of different temperatures on the dye adsorption performance of the SRB sludge, the experiments were carried out at 22, 35 and 50 °C at an initial dye concentration of 100 mg/L and initial pH of 3.5. Temperature affected biosorption to a lesser extent within the range of 22–50 °C. The biosorption of CR decreased slightly from 82.64 to 78.20 mg dye/g cell with increasing temperature from 22 to 50 °C (data are not shown here). These results indicate the exothermic nature of biosorption process of the dye on SRB sludge.

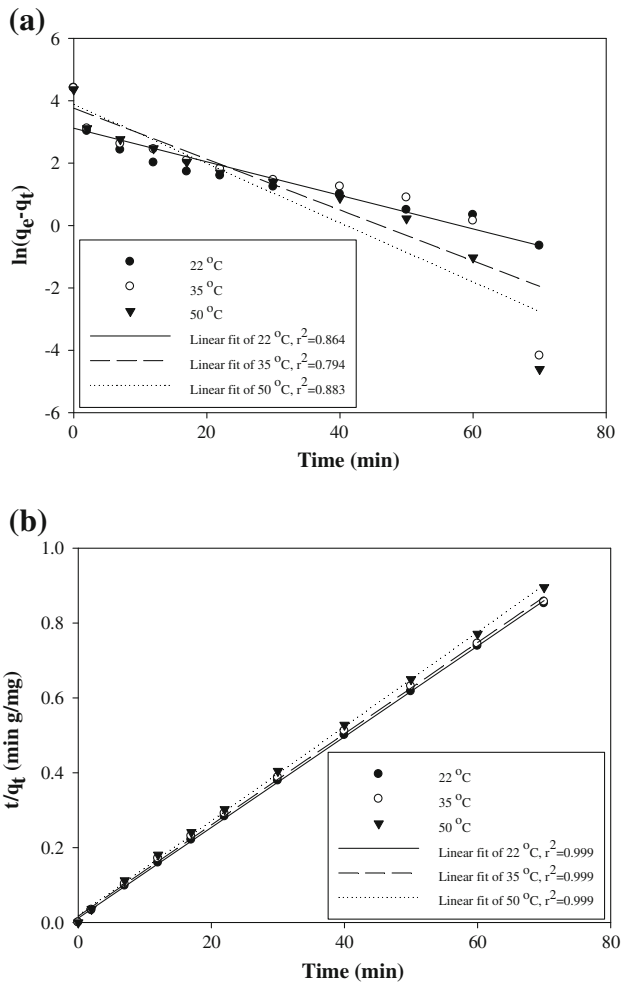

Fig. 2 Biosorption kinetics for the biosorption of CR by anaerobic SRB sludge **a** Pseudo-first-order model **b** pseudo-second-order model (initial pH = 3.5, 110 rpm, C_i = 100 mg/L)

Table 2 Pseudo-first- and pseudo-second-order rate constants for CR biosorption onto the anaerobic SRB sludge at different temperatures (22, 35, 50 °C, C_i = 100 mg/L, initial pH = 3.5, 110 rpm)

Temperature (°C)	First-order kinetics			Second-order kinetics			Experimental
	k_1	$q_{e,cal}$	r^2	k_2	$q_{e,cal}$	r^2	$q_{e,exp}$
22	0.054	22.60	0.864	0.013	82.81	0.999	82.64
35	0.082	42.88	0.794	0.0088	81.97	0.999	81.68
50	0.095	48.41	0.883	0.0083	79.36	0.999	78.21

The Gibbs energy ΔG^0, Enthalpy ΔH^0 and entropy ΔS^0 can be calculated from the following equations:

$$\Delta G^0 = -RT \ln K_c \quad (2)$$

where $K_c = q_e/C_e$

$$\ln K_c = \frac{\Delta S^0}{R} - \frac{\Delta H^0}{RT} \quad (3)$$

where ΔG^0, ΔH^0 and ΔS^0 are the standard free energy change, standard enthalpy change and standard entropy change, respectively, K_c is the equilibrium constant, q_e (mg dye/g cell) is the equilibrium concentration of the dye on the adsorbent, C_e (mg/L) is the equilibrium concentration of CR in solution, R is the ideal gas constant, and T (K) is the adsorption temperature. The ΔH^0 and ΔS^0 values were obtained from a linear plot of ln K_c versus $1/T$ (data not shown here). The equilibrium constant K_c and ΔG^0 changed from 4.09 to 3.20 and from −3.46 to −3.12 kJ/mol, respectively, with increasing temperature from 22 to 50 °C, which indicates the exothermic nature of CR adsorption on the SRB sludge. The negative value of ΔH^0 (−7.04 kJ/mol) shows that the heat was released during adsorption, indicating the exothermic nature of biosorption. The negative ΔS^0 value (−11.95 J/mol K) showed a decrease in randomness at the dye/sludge interface during the biosorption of CR on the SRB sludge.

Adsorption kinetics

A pseudo-first-order model was applied to fit the experimental data and evaluate the adsorption kinetics of CR on anaerobic SRB sludge (Lagergren 1898). The Lagergren pseudo-first-order model suggests that the rate of sorption is proportional to the number of sites unoccupied by the solutes. The pseudo-first-order model can be written in linearized form as follows:

$$\ln(q_e - q_t) = \ln q_e - k_1 t \quad (4)$$

where q_t is the dye concentrations (mg/g) at any time (t) and k_1 is the first-order rate constant (min^{-1}). Figure 2a shows a plot of $\ln(q_e - q_t)$ versus t at different reaction temperatures. The pseudo-first-order model did not fit the entire range of the adsorption process well and was only applicable over the initial contact times. The Lagergren first-order rate constant (k_1) and equilibrium dye concentration (q_e) values were calculated from the model (Table 2).

The adsorption data were then analyzed using the pseudo-second-order kinetic model (McKay and Ho 1999). The pseudo-second-order kinetic model can be written in linearized form as follows:

$$\frac{t}{q_t} = \frac{1}{k_2 q_e^2} + \frac{t}{q_e} \quad (5)$$

where k_2 is the second-order rate constant (g/mg min). By plotting t/q_t versus t, straight lines were obtained for different reaction temperatures (Fig. 2b). The values of the regression coefficient were quite high ($r^2 > 0.998$) and the experimental q_e values were in good agreement with the theoretical values calculated from the pseudo-second-order equation (Table 2). The pseudo-second-order kinetic model provides a better correlation for the adsorption of CR on the SBR sludge at different temperatures compared to the pseudo-first-order model. Therefore, the rate-limiting step in the biosorption process

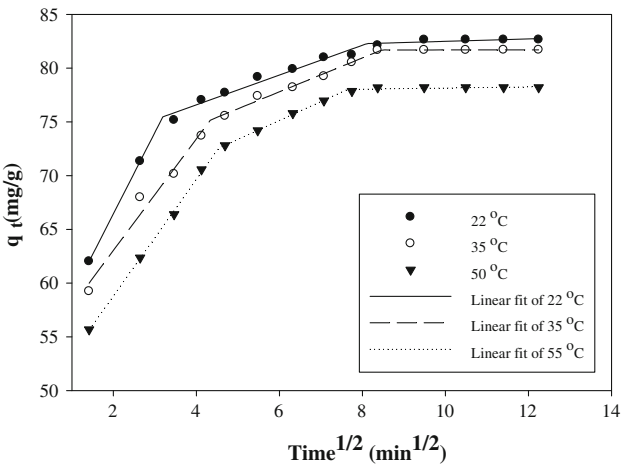

Fig. 3 Intraparticle diffusion model for the biosorption of CR by anaerobic SRB (initial pH = 3.5, 22, 35, 50 °C, 110 rpm, C_i = 100 mg/L)

Table 3 Intraparticle diffusion model rate constants for CR biosorption of CR onto anaerobic SRB sludge at different temperatures (22, 35, 50 °C, C_i = 100 mg/L, initial pH = 3.5, 110 rpm)

Temperature (°C)	1st linear portion			2nd linear portion			3rd linear portion		
	k_{i1}	r^2	C	k_{i2}	r^2	C	k_{i3}	r^2	C
22	7.536	0.999	51.36	1.382	0.977	71.08	0.046	0.847	82.14
35	5.212	0.977	52.60	1.580	0.991	68.30	0.0152	0.846	81.62
50	5.084	0.991	48.74	1.937	0.973	63.18	0.0123	0.862	78.06

is the chemical interactions between the functional groups of biosorbent and dye ions.

On the other hand, the pseudo-second-order model does not identify the diffusion mechanism. Therefore, the kinetic data were used to examine the presence or absence of intraparticle diffusion and determine whether intraparticle diffusion was the rate-limiting step. The Weber–Morris intraparticle diffusion model is commonly expressed using the following equation (Weber and Morris 1963):

$$q_t = k_i t^{1/2} + C \tag{6}$$

where k_i is the intraparticle diffusion rate constant (mg/g min) and C (mg/g) is the intercept. Intraparticle diffusion is the sole rate-limiting step if the plot of q_t versus $t^{1/2}$ is linear and passes through the origin (Ozcan and Ozcan 2005). Figure 3 presents a plot of the CR adsorption density (mg/g) as a function of $t^{1/2}$ at an initial dye concentration of 100 mg/L and at different temperatures. The plot was not linear over the entire time range, suggesting that more than one mode of adsorption occurred in the uptake of CR by the SRB sludge. This could be separated into three linear regions. The initial linear portion might be due to external surface adsorption, in which the dye diffused through the solution to the external surface of the adsorbent, and the uptake rate was quite high. The intermediate linear portion refers to gradual adsorption due to intraparticle diffusion in the macro-, meso- and micropores. Thereafter, the final linear portion corresponds to very slow and stable adsorption, approaching the equilibrium stage. Similar results were obtained for the removal of CR by ball-milled bagasse from an aqueous solution (Zhang et al. 2011). The intraparticle diffusion rate constants were calculated from the slope of the multi-linear plots at different temperatures (Table 3). Table 3 shows that the external mass transfer rate (k_{i1}) at the first linear portion was much higher than the intraparticle diffusion rate (k_{i2}) and equilibrium adsorption rate (k_{i3}) at the second and final linear portions, respectively. The values of the intercept C in the second linear portion (intraparticle diffusion) provide information on the thickness of the boundary layer. The boundary layer thickness decreased by increasing temperature (Table 3). This suggests that surface diffusion is more important at high temperatures because of the greater random motion associated with the increased thermal energy.

Biosorption isotherms

The equilibrium distribution of CR between the adsorbent and liquid phase is important for determining the maximum adsorption capacity of the SRB sludge for CR and understanding the mechanism of adsorption. In this study, nonlinear and linearized forms of three different adsorption models, such as Langmuir, Freundlich and Tempkin isotherms, were investigated to examine the experimental data.

The Langmuir isotherm model assumes that adsorption takes place at specific homogeneous sites on the surface of the adsorbent, suggesting that once a dye molecule occupies a site, no further adsorption can take place at that site. The nonlinear expression of Langmuir adsorption isotherm can be given as (Langmuir 1918):

$$q_e = \frac{q_{max} K_L C_e}{1 + K_L C_e} \tag{7}$$

where q_{max} (mg dye/g cell) is the maximum biosorption capacities of the adsorbent and K_L (L/mg) is the Langmuir constant related to the free energy of biosorption. Equation (7) of Langmuir isotherm can be linearized as the following equation:

$$\frac{1}{q_e} = \frac{1}{q_{max}} + \frac{1}{q_{max} K_L C_e} \tag{8}$$

The Freundlich equation based on adsorption on a heterogeneous surface is given as (Freundlich 1906):

$$q_e = K_F C_e^{\frac{1}{n}} \tag{9}$$

where K_F (L/g) is the Freundlich constant related to the biosorption capacity of the biosorbent and

Table 4 Comparison of linearized and nonlinearized isotherms for the biosorption of CR onto SRB sludge (22 °C, initial pH = 3.5, 110 rpm)

Isotherm	Calculated isotherm parameters	χ^2	APE	r^2
Linearized				
Langmuir	q_{max} = 263.16 mg/g, K_L = 0.014 L/mg	2.68	4.29	0.986
Freundlich	K_F = 33.71 L/g, n = 3.51	25.31	15.28	0.810
Tempkin	A = 0.26 L/g, b = 51.92	7.52	8.52	0.967
Nonlinearized				
Langmuir	q_{max} = 266.14 mg/g, K_L = 0.013 L/mg	2.43	3.91	0.990
Freundlich	K_F = 33.88 L/g, n = 3.27	13.42	11.87	0.933
Tempkin	A = 0.17 L/g, b = 47.39	2.58	4.44	0.981

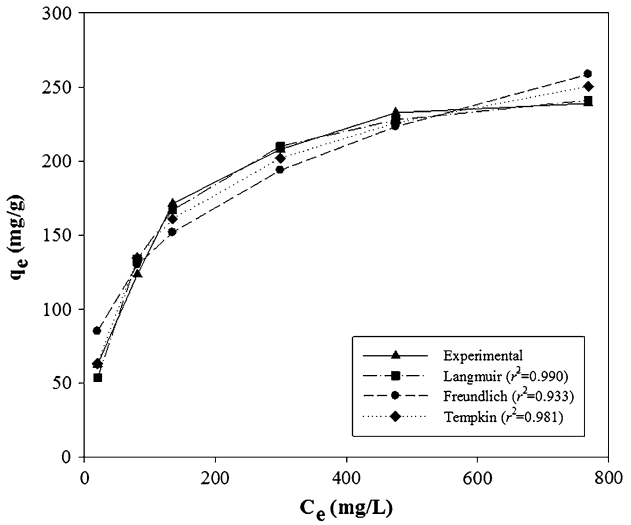

Fig. 4 Nonlinear isotherm models for CR biosorption by anaerobic SRB sludge (initial pH = 3.5, 22 °C, 110 rpm)

n (dimensionless) is Freundlich exponent indicating the biosorption intensity. The Freundlich model did not consider biosorbent saturation. Equation (9) of Freundlich isotherm can be linearized by taking logarithms as the following equation:

$$\ln q_e = \ln K_F + \frac{1}{n} \ln C_e \quad (10)$$

The Tempkin isotherm assumes that the biosorption energy during the biosorption process decreases linearly with increasing saturation of biosorption sites rather than decreasing exponentially, as implied by the Freundlich isotherm. The Tempkin isotherm is given as (Tempkin and Pyzhev 1940):

$$q_e = \frac{RT}{b \ln (AC_e)} \quad (11)$$

Equation (11) of Tempkin isotherm can be linearized as:

$$q_e = B \ln A + B \ln C_e \quad (12)$$

where $B = RT/b$, b is the Tempkin constant related to the biosorption energy, A is the equilibrium binding constant (L/mg) and B is constant related to the heat of sorption.

To evaluate the fitness of the isotherm equations, Chi square (χ^2) and average percentage errors (APE) were calculated from the following equations (Ho and Wang 2004; Subramanyam and Das 2009):

$$\chi^2 = \sum \frac{(q_{e,calc} - q_{e,exp})^2}{q_{e,exp}} \quad (13)$$

$$APE = \frac{100}{n} \sum \left| \frac{(q_{e,calc} - q_{e,exp})}{q_{e,exp}} \right| \quad (14)$$

where n is the number of observations, $q_{e,exp}$ and $q_{e,calc}$ are the experimental and calculated values, respectively.

The linearized and nonlinearized isotherms' coefficients were estimated using either graphical methods or nonlinear regression method (Matlab 7.8). Table 4 shows the comparison of linearized and nonlinearized isotherms in terms of χ^2, APE and correlation coefficient (r^2). All the nonlinearized models give lower APE and χ^2 values than the corresponding linearized models. This clearly indicates that it is better to find isotherm coefficients by nonlinear models. Among the nonlinear models, the Langmuir

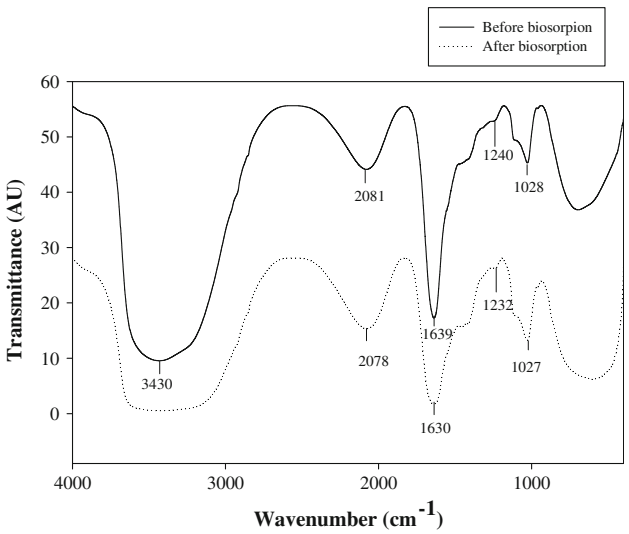

Fig. 5 FTIR spectra of SRB sludge **a** before and **b** after dye biosorption

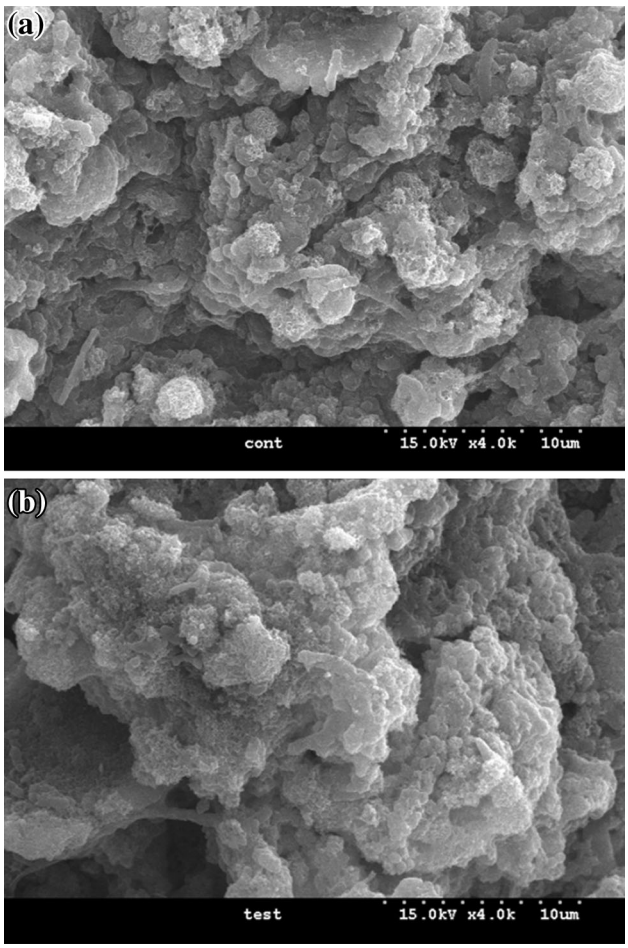

Fig. 6 SEM images of **a** control SRB sludge **b** dye loaded SRB sludge

isotherm gives the equilibrium adsorption data better than the Freundlich and Tempkin isotherms, which were confirmed by the high r^2 value (Fig. 4). The maximum adsorption capacity (q_{max}) of the SRB sludge for CR was 238.90 dye/g cell at an initial dye concentration of 1,000 mg/L, which is in line with the theoretically calculated value of 266.14 mg dye/g cell using the nonlinear Langmuir model.

The Langmuir constant K_L can be used to determine the biosorption equilibrium behavior using the Hall separation factor R_L (dimensionless) (Hall et al. 1966):

$$R_L = \frac{1}{(1 + R_L C_i)} \quad (15)$$

where C_i is the highest initial dye concentration in mg/L. The R_L value indicates the type of isotherm to be either irreversible ($R = 0$), linear ($R_L = 1$), unfavorable ($R_L > 1$) or favorable ($0 < R_L < 1$). The R_L values calculated from the experimental data were between 0 and 1, indicating that CR adsorption on the SRB sludge is favorable.

FTIR analysis and SEM images

Figure 5 shows the FTIR spectrum of the SRB sludge before and after the biosorption of CR dye. The peak at 3,435 cm^{-1} after dye biosorption became broadened, indicating the involvement of an NH group in biosorption. The strong and broad band ranging from 3,600 to 3,200 cm^{-1} was assigned to an overlapping of the O–H and N–H stretching vibrations (Panda et al. 2008; Sun et al. 2009). Moreover, obvious displacements were observed at 1,639–635 cm^{-1} and 1,240–1,232 cm^{-1}, suggesting that the biosorption involved C = C stretching (–CH = CH–) and S = O stretching vibrations (Ding et al. 2012; Elangovan et al. 2008). Figure 6 shows SEM images of the SRB sample before and after CR adsorption. The surface morphology of the SRB sludge before adsorption clearly shows that a considerable number of heterogeneous layers of pores are available for CR adsorption. Significant changes in the surface morphology after CR adsorption were observed. The external surface of the SRB sludge was covered mostly with the CR dye.

Conclusion

Activated sulfidogenic sludge was isolated from anaerobic digester sludge, and the biosorption of CR from an aqueous solution was investigated. The SRB sludge showed a high biosorption density with equilibrium adsorption being achieved practically in 70 min. The removal of CR dye from the aqueous solution depended strongly on the pH of the solution, the initial dye concentration and contact time. The kinetic results showed that the pseudo-second-order kinetic model gave the best correlation coefficient and agreed with the calculated equilibrium dye concentration (qe) and experimental values. The Langmuir isotherms were found to provide a better fit to the experimental data than the Freundlich and Tempkin models. The thermodynamic parameters suggested the spontaneous and exothermic nature of CR biosorption on the anaerobic SRB sludge. The dye biosorbent interactions were verified by FTIR spectroscopy. In addition, SEM confirmed that the heterogeneous and porous sludge structure of the SRB sludge is suitable for dye biosorption. Overall, the low cost, high adsorption capacity and successful application for the removal of CR dye from aqueous solutions confirmed the applicability of SRB sludge.

Acknowledgments This research was supported by Basic Science Research Program through the National Research Foundation of Korea (NRF) funded by the Ministry of Education, Science and Technology (MEST) (2010-0023442). This study was also supported by the Priority Research Centers Program through an NRF grant funded by MEST (2010-0028301).

References

Acemioğlu B (2004) Adsorption of Congo Red from aqueous solution onto calcium-rich fly ash. J Colloid Interface Sci 274:371–379

APHA (1998) Standard methods for the examination of water and wastewater, 20th ed. APHA, AWWA, WPCF. American Public Health Association, Washington, DC

Bonancêa CE, do Nascimento GM, de Souza ML, Temperini MLA, Corio P (2006) Substrate development for surface-enhanced Raman study of photocatalytic degradation processes: Congo Red over silver modified titanium dioxide films. Appl Catal B 69:34–42

Caner N, Kiran I, Ilhan S, Iscen CF (2009) Isotherm and kinetic studies of Burazol Blue ED dye biosorption by dried anaerobic sludge. J Hazard Mater 165:279–284

Chatterjee S, Chatterjee S, Chatterjee BP, Guha AK (2007) Adsorptive removal of Congo Red, a carcinogenic textile dye by Chitosan hydrobeads: binding mechanism, equilibrium and kinetics. Colloids Surf A 299:146–152

Ding Y, Jing D, Gong H, Zhou L, Yang X (2012) Biosorption of aquatic cadmium (II) by unmodified rice straw. Bioresour Technol 114:20–25

Elangovan R, Philip L, Chandraraj K (2008) Biosorption of chromium species by aquatic weeds: kinetics and mechanism studies. J Hazard Mater 152:100–112

Freundlich HMF (1906) Over the adsorption in solution. J Phys Chem 57:385–470

Hall KR, Eagleton LC, Acrivos A, Vermeulen T (1966) Pore and solid-diffusion kinetics in fixed-bed adsorption under constant-pattern conditions. Ind Eng Chem Fundam 5:212–223

Han R, Ding D, Xu Y, Zou W, Wang Y, Li Y, Zou L (2008) Use of rice husk for the adsorption of Congo Red from aqueous solution in column mode. Bioresour Technol 99:2938–2946

Ho YS, Wang CC (2004) Pseudo-isotherms for the sorption of cadmium ion onto tree fern. Proc Biochem 39:761–765

Isik M, Sponza DT (2005) Effects of alkalinity and co substrate on the performance of an upflow anaerobic sludge blanket (UASB) reactor through decolorization of Congo Red azo dye. Bioresour Technol 96:633–643

Ju DJ, Byun IG, Park J, Lee CH, Ahn GH, Park TJ (2008) Biosorption of a reactive dye (Rhodamine-B) from an aqueous solution using dried biomass of activated sludge. Bioresour Technol 99:7971–7975

Lagergren S (1898) Zur theorie der sogenannten adsorption gelöster stoffe Kungliga Svenska Vetenskapsakademiens. Handlingar 24:1–39

Langmuir I (1918) The adsorption of gases on plane surfaces of glass, mica and platinum. J Am Chem Soc 40:1361–1403

Lian L, Guo L, Guo C (2009) Adsorption of Congo Red from aqueous solutions onto Ca-bentonite. J Hazard Mater 161:126 –131

McKay G, Ho YS (1999) Pseudo second order model for sorption processes. Process Biochem 34:451–465

Namasivayam C, Muniasamy N, Gayathri K, Rani M, Ranganathan K (1996) Removal of dyes from aqueous solutions by cellulosic waste orange peel. Bioresour Technol 57:37–43

Ofomaja AE, Naidoo EB, Modise SJ (2009) Removal of copper (II) from aqueous solution by pine and base modified pine cone powder as biosorbent. J Hazard Mater 168:909–917

Otero M, Rozada F, Calvo L, Garcia AI, Moran A (2003) Elimination of organic water pollutants using adsorbents obtained from sewage sludge. Dyes Pigm 57:55–65

Ozcan A, Ozcan AS (2005) Adsorption of Acid Red 57 from aqueous solutions onto surfactant modified sepiolite. J Hazard Mater 125:252–259

Panda GC, Das SK, Guha AK (2008) Biosorption of cadmium and nickel by functionalized husk of *Lathyrus sativus*. Colloids Surf B 62:173–179

Postgate JR (1984) The sulphate-reducing bacteria, 2nd edn. Cambridge University Press, Cambridge

Qiu B, Xiang C, Dezhi S (2012) Characteristics of cationic Red X-GRL biosorption by anaerobic activated sludge. Bioresour Technol 113:102–105

Rasool K, Woo SH, Lee DS (2013) Simultaneous removal of COD and Direct Red 80 in a mixed anaerobic sulfate-reducing bacteria culture. Chem Eng J 223:611–616

Saha PD, Chowdhury S, Mondal M, Sinha K (2011) Biosorption of direct red 28 (Congo Red) from aqueous solutions by eggshells: batch and column studies. Sep Sci Technol 47:112–123

Sara D, Tushar KS (2012) Removal of anionic dye Congo Red from aqueous solution by raw pine and acid-treated pine cone powder as adsorbent: equilibrium, thermodynamic, kinetics, mechanism and process design. Water Res 46:1933–1946

Senthil K, Ramalingam P, Senthamarai S, Niranjanaa C, Vijayalakshmi M, Sivanesan PS (2010) Adsorption of dye from aqueous solution by cashew nut shell: studies on equilibrium isotherm, kinetics and thermodynamics of interactions. Desalination 261:52–60

Somasekhara RMC, Sivaramakrishna L, Varada RA (2012) Use of an agricultural waste material, Jujuba seeds for the removal of anionic dye (Congo Red) from aqueous medium. J Hazard Mater 203–204:118–127

Subramanyam B, Das A (2009) Linearized and non-linearized isotherm models comparative study on adsorption of aqueous phenol solution in soil. Int J Enviorn Sci Tech 6:640

Sun XF, Wang SG, Zhang XM, Chen JP, Li XM, Gao BY, Ma Y (2009) Spectroscopic study of Zn^{2+} and Co^{2+} binding to extracellular polymeric substances (EPS) from aerobic granules. J Colloid Int Sci 335:11–17

Tempkin MI, Pyzhev V (1940) Kinetics of ammonia synthesis on promoted iron catalyst. Acta Phys Chim USSR 12:327–356

Toor M, Jin B (2012) Adsorption characteristics, isotherm, kinetics, and diffusion of modified natural bentonite for removing diazo dye. Chem Eng J 187:79–88

Vimonses V, Lei S, Jin B, Chow C, Saint C (2009) Adsorption of Congo Red by three Australian kaolins. Appl Clay Sci 43:465–472

Wang Y, Mu Y, Zhao Q, Yu H (2006) Isotherms, kinetics and thermodynamics of dye biosorption by anaerobic sludge. Sep Purif Technol 50:1–7

Weber WJ, Morris JC (1963) Kinetics of adsorption on carbon from solution. J Sant Eng Div ASCE 89:31–59

Weisburger JH (2002) Comments on the history and importance of aromatic and heterocyclic amines in public health. Mutation Res 30:9–20

Zhang Z, Moghaddam L, Ian M, Doherty OS (2011) Congo Red adsorption by ball-milled sugarcane bagasse. Chem Eng J 178:122–128